DENTAL MATERIALS 33 (2017) 288–293

Available online at www.sciencedirect.com

ScienceDirect

journal homepage: www.intl.elsevierhealth.com/journals/dema

Application of close-packed structures in dental resin composites

*Ruili Wang, Eric Habib, X.X. Zhu**

Département de Chimie, Université de Montréal, C.P. 6128, Succursale Centre-ville, Montreal, QC, H3C 3J7, Canada

ARTICLE INFO

Article history:
Received 31 July 2016
Received in revised form
9 December 2016
Accepted 14 December 2016

Keywords:
Spherical particles
Close-packed structures
The packing factor
Filler formulations
Dental resin composites

ABSTRACT

Objective. The inorganic filler particles in dental resin composites serve to improve their mechanical properties and reduce polymerization shrinkage during their use. Efforts have been made in academia and industry to increase the filler particle content, but, few studies examine the theoretical basis for the maximum particle loading.

Methods. This work evaluates the packing of spherical particles in a close-packed state for highly loaded composites.

Results. Calculations show that for low dispersity particles, the maximum amount of particles is 74.05 vol%, regardless of the particle size. This can be further improved by using a mix of large and small particles or by the use of non-spherical particles. For representative spherical particles with a diameter of 1000 nm, two types of secondary particles with respective sizes of 414 nm (d_I) and 225 nm (d_{II}) are selected. The results show that after embedding secondary particles **I & II** into primary spherical particles, the packing factor is increased to 81.19% for the close-packed structures, which shows an improvement of 9.64%, compared to the 74.05% obtained only with primary spherical particles. This packing factor is also higher than either structure with the embedded secondary particles **I or II**.

Significance. Examples of these mixtures with different spherical particle sizes are shown as a theoretical estimation, serving as a guideline for the design and formulation of new dental resin composites with better properties and improved performance.

1. Introduction

Dental resin composites are mainly comprised of an organic matrix mixed with silanized inorganic fillers, and can be cured to form a crosslinked composite polymer network with the blue light irradiation [1]. While the resin phase contributes to the toughness of the composites related to the mechanical strength in flexure or tension, their mechanical properties in regard to their modulus and hardness, are dominated by the filler particles for the similar resin matrices [2,3]. Recent research efforts have been aimed at optimizing filler formulations including filler loading, size, and morphology, with the aim of improving mechanical properties and reducing polymerization shrinkage during their clinical use [4–6]. These results have shown that higher loading fractions in resin composite have led to materials with superior mechanical properties. For filler formulations with larger particles, the addition of smaller particles, either spherical or irregular, could improve fracture toughness, shrinkage strain, and wear behavior of the resulting composites [7–9]. However, in previous reports, authors show series of filler formulations where the reason for choosing them is seldom mentioned [7–9]. Few studies examine the theoretical basis for the maximum particle loading in a resin composite [10]. Therefore, it is desirable and useful to develop a model for the refinement of filler formulations without trial and error.

This model in this paper is based on the theory of close-packed structures of spherical particles of identical sizes for

* *Corresponding author.*
E-mail address: julian.zhu@umontreal.ca (X.X. Zhu).

http://dx.doi.org/10.1016/j.dental.2016.12.006

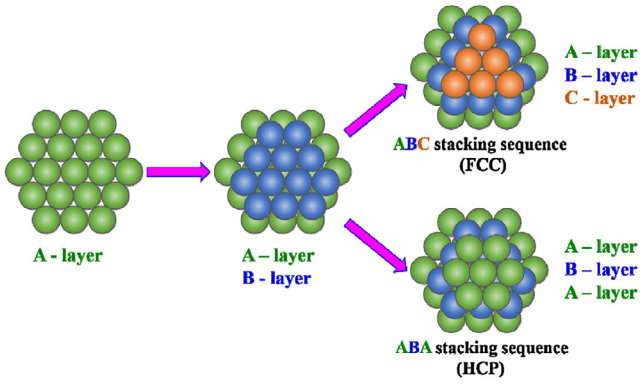

Fig. 1 – Stacking sequences of face-centered cubic (FCC) arrangement and hexagonal close-packed (HCP) arrangement.

the refinement of filler formulations with the aim to estimate the maximum allowed loading of the particles.

2. Methods

2.1. *Particle packing theory*

The following particle optimizations are based on previous work on systems modeling the packing of identical spheres. Most of the previous work was first explored in the context of crystal structures, which showed that atoms tend to arrange in certain patterns, or lattice arrangements, the most efficient of which are known as close-packed structures. These are modeled with a unit cell that is repeated in all directions for the purpose packing, though in some cases boundary conditions may need to be defined. The two close-packed arrangements with the highest packing efficiency are called face centered cubic (FCC) and hexagonal close packed (HCP) [11,12]. Their stacking arrangements and unit cells are shown in Figs. 1 and 2, respectively. While most of the work on packing structures applies to atoms or nanoparticles (on the order of 10 nm) [13], the lower mobility of larger particles such as those used for dental composites may not allow effective FCC and HCP arrangements, resulting in random packing orders. For the purpose of modeling voids in the structures, FCC and HCP arrangements are used since they are the most appropriate.

In the literature, the particle loading for dental resin composites is most often quoted as the mass fraction of the particles with respect to the total mass of the final product. Since the density of the filler in dental materials is much higher than that of the resin, typically on the order of 2.2 g/cm^2 for silica [14] vs 1.161 g/cm^2 for bisphenol A glycerolate dimethacrylate (Bis-GMA) [15], the weight fraction is higher than the volume fraction for the filler loading. In the context of sphere packing, the packing factor instead refers to the volume fraction occupied by particles in the unit cell, which is defined as [11]:

$$\text{Packing factor} = V_s/V_c \quad (1)$$

where V_s is the volume of all the spheres in a unit cell (assuming the hard sphere model), and V_c is the total volume of a unit cell.

2.1.1. *FCC*

The FCC arrangement is based on a cubic unit cell with particles located at each of the corners and at the centers of each the square face [11], as shown in Fig. 2(a–c). As previously studied, a total of four whole particles can be assigned to a FCC unit cell (Table 1), therefore, their occupied volume can be defined as $V_s = \left(4 \times \frac{4\pi}{3} R^3\right)$, where R is the radius of particles. The total volume of the unit cell is computed as $V_c = a^3$, where a is the length of the unit cell (Fig. 3a). Following simplification, the unit cell size a and the particle radius R cancel out, resulting in a size-independent packing factor of $\frac{\sqrt{2}\pi}{6}$, or approximately 74.05% [16–18].

2.1.2. *HCP*

Similarly, the HCP arrangement is based on a stacked hexagonal arrangement of particles, with a particle at each vertex of the hexagon, in addition to one in the center. Two of these are stacked with an intervening layer that provides three additional particles (Fig. 2d–f) [11]. Still using particles of radius R, and seeing a total of six whole particles for a unit cell (Table 1), thus $V_s = \left(6 \times \frac{4\pi}{3} R^3\right)$, and $V_c = \left(6 \times \frac{1}{2} \times \frac{\sqrt{3}}{2} a^2 \times c\right)$, where a and c represent the short and long unit cell dimensions, and calculations yield the same value as FCC, with an identical packing factor of 74.05% (Fig. 3b) [17,18].

The above results indicate that, regardless of particle size, even in the most efficient packing arrangements, identical spheres cannot completely fill the space. There are necessarily voids between particles; these voids have complex shapes, however for filler loading purposes, we are mostly interested in the largest spherical particles which can fit into these voids. In the close-packed structures discussed above, two types of voids are formed, tetrahedral voids and octahedral voids, which are identical in both FCC and HCP as the voids exist between two layers of atoms (Fig. 4) [19]. However, the number of voids in these close-packed structures is different, which will be addressed further. Previous work has also shown that the maximum diameter of a tetrahedral void (d_4) is 0.45 R, whereas that of an octahedral void (d_8) is 0.828 R, where R is the radius of the packed spheres, as derived from the close packing sphere models [20].

2.1.3. *RCP*

While FCC and HCP are the most efficient packing arrangements, many more exist, such as simple cubic and body centered cubic (BCC) [11,21]; their detailed information including coordination numbers, number of particles per unit cell, and packing efficiency are collected in Table 1 [21,22]. However, these fully ordered models assume frictionless interactions between the particles, such that diffusion is very fast on the scale of the particles. In order to model systems in which friction is a non-negligible force and particle diffusion is slow, random packing is considered. When a set of spheres is put into a packed state, a random packed arrangement will generally result, and there exists a range of random-packing packing factors, with an upper limit of 64% and a lower limit of 55%

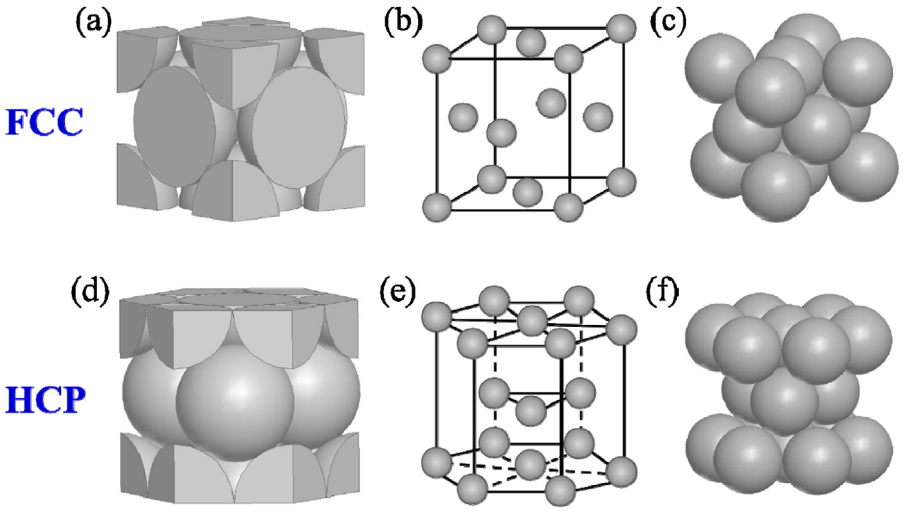

Fig. 2 – The unit cells of FCC and HCP arrangements; there are three representations for each: a space-filling cutaway model that shows the portion of each atom that lies within the unit cell (a, d), a ball-and-stick model (b, e), and an arrangement of atoms in a unit cell (c, f).

Table 1 – Comparison of various models of close sphere packing arrangements.

Unit cell	Abbrev.	Coordination number[a]	Number of particles per unit cell	Approximate packing efficiency (%)
Simple cubic	/	6	1	52
Body centered cubic	BCC	8	2	68
Face centered cubic	FCC	12	4	74
Hexagonal close packed	HCP	12	6	74
Random close packed	RCP	6	/	64
Random loose packed	RLP	4	/	55

[a] Coordination number: the number of inter-particle contacts per atom [10].

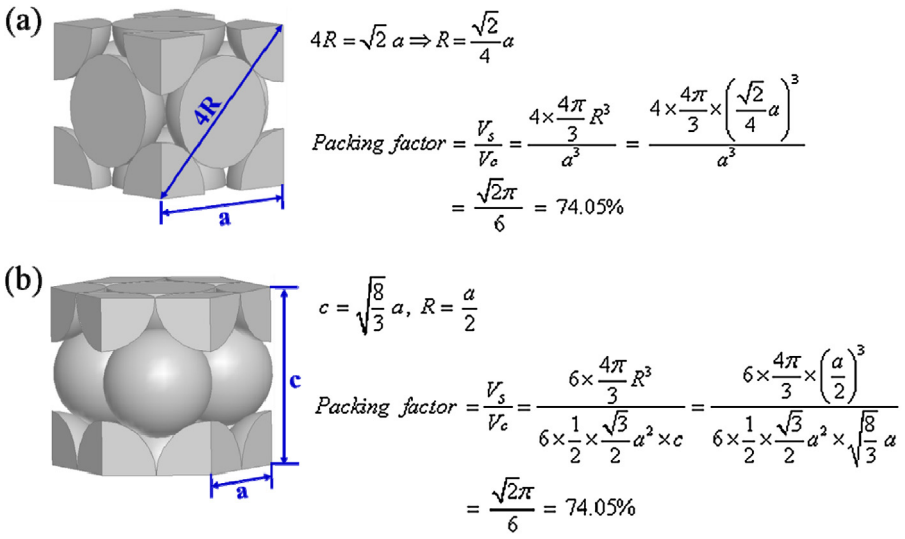

Fig. 3 – Calculation of the packing factor of FCC arrangement (a), and HCP arrangement (b).

[23,24]. The upper limit is often referred as random close packed (RCP), and the lower limit as random loose packed (RLP) [25].

RCP in three dimensions has been studied experimentally by shaking containers full of steel ball bearings and extrapolating the measured densities to eliminate finite-size effects [26,27]. RLP is a less well-defined concept than RCP,

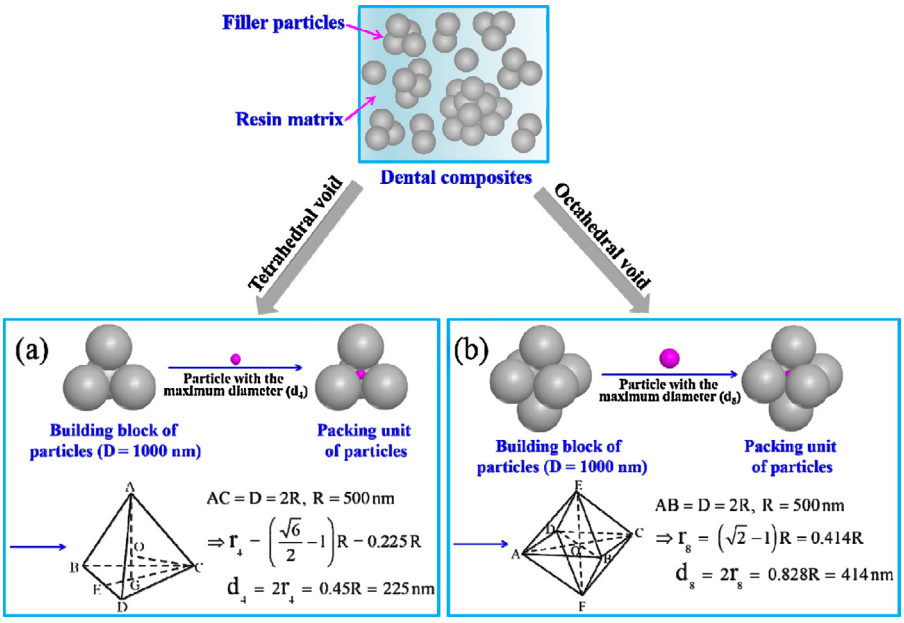

Fig. 4 – Representative calculation of the maximum size of spherical particles fit into a tetrahedral void (a), and an octahedral void (b), based on the close packing of identical sphere particles (D = 1000 nm).

and represents the loosest possible random packing that is mechanically stable [25,26]. The empirically derived RCP and RLP have coordination numbers of 6 and 4, respectively [28].

3. Results

3.1. *Application to 1000 nm particle system*

FCC and HCP models are used to mathematically investigate the effect of secondary particle size on the packing factors of systems of close-packed spherical particles. Here, we give a representative example where the largest spherical particles have a diameter of 1000 nm (D = 1000 nm). The calculation of d_4 and d_8 is shown in Fig. 4. The theoretical void sizes d_4 and d_8 are 225 nm and 414 nm, respectively. These theoretical calculations give us a better understanding of the effect of particle compositions, and can be used to optimize the filler formulations for dental resin composites.

3.2. *Theoretical packing factor*

Here, we select two types of secondary particles with sizes of 414 nm (d_I) and 225 nm (d_{II}), respectively, which correspond to d_8 and d_4 of the 1000 nm primary spherical particles, as discussed above. The effect of these two smaller embedded spherical particles on the packing factor of the packed mixture is calculated with Formula (2) and investigated below.

$$\text{Packingfactor} = \frac{Vs + V4 + V8}{Vc} \quad (2)$$

where V_s is the volume of the packed primary spherical particles in a unit cell, V_4 is the volume of the embedded spherical particles in tetrahedral voids, V_8 is the volume of the embedded spherical particles in octahedral voids, V_c is the total volume of a unit cell.

3.2.1. *Secondary spherical particles I*

If using secondary spherical particles d_I of a size matching the octahedral voids d_8 for the 1000 nm primary spherical particles, they will fit only into the octahedral voids, but not the smaller tetrahedral voids. Thus four particles can be embedded into an FCC structure or six into a HCP structure, on the basis of the number of voids [29,30], and the corresponding V_8 are shown in Table 2. Additionally, V_s and V_c for FCC and HCP can be calculated from Fig. 3. Then, the packing factor of these two arrangements after embedding the secondary spherical particles I can both be simplified as the following Formula (3):

$$\text{Packingfactor} = \frac{\pi\left(R^3 + {r_I}^3\right)}{3\sqrt{2}R^3} \quad (3)$$

where R is the radius of primary spherical particles, r_I is the radius of secondary spherical particles I.

Using 500 nm for R and 207 nm for r_I in the above Formula (3), it can be observed that the packing factors of both FCC and HCP are increased to 79.50%, as shown in Table 2. This is an improvement of 7.36%, compared with the 74.05% packing factor without adding secondary spherical particles.

3.2.2. *Secondary spherical particles II*

Secondary spherical particles II of a size corresponding to the tetrahedral voids (d_4) of the 1000 nm primary spherical particles will fit into both tetrahedral voids and octahedral voids of FCC or HCP arrangements. Each void is considered to be filled with only a single particle. Consequently, according to the analysis of the number of voids [29,30], V_4 and V_8 in a FCC or HCP unit cell are also shown in Table 2. V_s and V_c of these

Table 2 – Collection of the number and the volume of tetrahedral and octahedral voids in a unit cell of FCC and HCP of primary spherical particles, and their packing factor after being fit into different secondary spherical particles.

Unit cell models	Number of tetrahedral voids	Number of octahedral voids	V_4	V_8	Packing factor (%)
No secondary spherical particles					
FCC	8	4	/	/	74.05
HCP	12	6	/	/	74.05
Secondary spherical particles I ($d_I = 414$ nm)					
FCC	8	4	/	$4 \times \frac{4\pi}{3} r_I^3$	79.50
HCP	12	6	/	$6 \times \frac{4\pi}{3} r_I^3$	79.50
Secondary spherical particles II ($d_{II} = 225$ nm)					
FCC	8	4	$8 \times \frac{4\pi}{3} r_{II}^3$	$4 \times \frac{4\pi}{3} r_{II}^3$	76.77
HCP	12	6	$12 \times \frac{4\pi}{3} r_{II}^3$	$6 \times \frac{4\pi}{3} r_{II}^3$	76.77
Secondary spherical particles I & II ($d_I = 414$ nm & $d_{II} = 225$ nm)					
FCC	8	4	$8 \times \frac{4\pi}{3} r_{II}^3$	$4 \times \frac{4\pi}{3} r_I^3$	81.19
HCP	12	6	$12 \times \frac{4\pi}{3} r_{II}^3$	$6 \times \frac{4\pi}{3} r_I^3$	81.19

two arrangements are shown in Fig. 3. Therefore, the packing factor of FCC or HCP arrangement after having the secondary particles d_4 embedded into them are also calculated from Formula (2) and simplified as Formula (4). The packing factor obtained is increased to 76.77% for both arrangements, which is an improvement of 3.67%, when compared to the 74.05% obtained without secondary particles, and also lower than the structure with the embedded d_8 particles shown above.

$$\text{Packingfactor} = \frac{\pi\left(R^3 + 3r_{II}^3\right)}{3\sqrt{2}R^3} \quad (4)$$

where R is the radius of primary spherical particles, r_{II} is the radius of secondary spherical particles **II**.

3.2.3. *Secondary spherical particles I & II*

For the sake of theoretical estimate, we suppose that both secondary spherical particles **I & II** may be used at the ideal proportions to fit into the voids. In this ideal case, secondary spherical particles **I** will only fit into the octahedral voids of FCC or HCP arrangements, and secondary spherical particles **II** will fit into the remaining tetrahedral voids. Each void is considered to be filled with only one particle of the ideal size without any misplacement. Therefore, based on the number of voids discussed previously, V_4 and V_8 in a FCC or HCP unit cell are shown in Table 2. V_s and V_c for FCC and HCP are shown in Fig. 3. The packing factor after embedding the secondary particles **I & II** can be calculated from Formula (2) and simplified as Formula (5).

$$\text{Packingfactor} = \frac{\pi\left(R^3 + 2r_{II}^3 + r_I^3\right)}{3\sqrt{2}R^3} \quad (5)$$

where R is the radius of primary spherical particles, r_I and r_{II} are the radius of secondary spherical particles **I & II**.

The packing factor increases to 81.19% for both FCC and HCP arrangements, which shows an improvement of 9.64%, compared to the 74.05% obtained without any secondary particles. This packing factor is also higher than either structure with the embedded d_8 particles or d_4 particles analyzed above.

3.2.4. *Deviations from ideality and limitations*

The calculations and analyses presented herein portray dental resin composites as ideal, and more importantly static systems. They are derived from an arrangement of particles in colloidal crystal structures with full regularity and coordination. In actuality, given the practical requirement of composite pastes malleability, a certain amount of excess resin matrix must be included to allow the movement and rearrangement without breakage. Even under ideal conditions, a system packed to 74.05 vol% would be a solid material rather than a plastic paste, and so such a high loading would not be achievable in practice. In this study, the filler particles are considered non-interacting hard spheres. This approximation would be fairly accurate for large particles (>500 nm), where the surface–resin interactions are low, but becomes increasingly inaccurate as the filler surface area increases. In such cases, an exponential increase in composite paste viscosity causes composite processing and handling to become problematic [10,31].

A further limitation of this study is that we only analyze the two largest sizes of spherical particles that could fit into the tetrahedral and octahedral voids of the close-packed structures (FCC and HCP); these voids could also be filled using commensurately smaller particles.

4. Conclusion

In summary, a theoretical calculation method from first principles was used for the optimization filler formulations for dental resin composites, based on the close-packed structures of monodisperse spherical fillers. For a single spherical filler size, the maximum packing efficiency of identical spherical particles is approximately 74.05 vol%, regardless of the sphere size. This value may be further increased with the use of a mixture of large- and small-size particles. As a representative example, the calculations were applied to obtain the maximum size of secondary spherical particles which can fit into the tetrahedral voids and octahedral voids. The resulting packing factors after embedding the secondary spherical particles are shown, the best of which was 81.19% when using two secondary particles corresponding to the octahedral void size and the tetrahedral void size. These secondary fillers increased the packing factor by 9.64% compared with that of the primary

particles alone. This work shows the application of close-packed structures in optimizing filler formulations of dental resin composites, which could also find potential use in other particle-reinforced materials.

It should however be noted that the application of close-packed structures in filler formulations is an idealized model, and that random packing may be the real packing arrangement. In this estimation, we do not consider the variations in particle size and shape, and the wetting requirement of the resin monomers (resin types and weight fractions) for the close-packed fillers, and it is clear that in practice the filler packing may be affected by these factors. Our prospective work will be focused on designing a series of handleable dental composites with the optimized formulations discussed in this study, and we intend to further investigate the effect of secondary particle size on the packing factor and the physical-mechanical properties of the final resin composites, so as to evaluate all presented theoretical calculations in reality.

Acknowledgments

This work was financially supported by NSERC and CIHR (grant number: CHRPJ 385852-10), and Project of Shanghai International Science and Technology Cooperation Fund (grant number: #14520710200).

REFERENCES

[1] Habib E, Wang RL, Wang YZ, Zhu MF, Zhu XX. Inorganic fillers for dental resin composites: present and future. ACS Biomater Sci Eng 2016;2:1–11.
[2] Kim KH, Ong JL, Okuno O. The effect of filler loading and morphology on the mechanical properties of contemporary composites. J Prosthet Dent 2002;87:642–9.
[3] Masouras K, Silikas N, Watts DC. Correlation of filler content and elastic properties of resin-composites. Dent Mater 2008;24:932–9.
[4] Liu FW, Sun B, Jiang XZ, Aldeyab SS, Zhang QH, Zhu MF. Mechanical properties of dental resin/composite containing urchin-like hydroxyapatite. Dent Mater 2014;30:1358–68.
[5] Leprince J, Palin WM, Mullier T, Devaux J, Vreven J, Leloup G. Investigating filler morphology and mechanical properties of new low-shrinkage resin composite types. J Oral Rehabil 2010;37:364–76.
[6] Wang RL, Zhang ML, Liu FW, Bao S, Wu TT, Jiang XZ, et al. Investigation on the physical-mechanical properties of dental resin composites reinforced with novel bimodal silica nanostructures. Mater Sci Eng C 2015;50:266–73.
[7] Elbishari H, Silikas N, Satterthwaite J. Filler size of resin-composites, percentage of voids and fracture toughness: is there a correlation? Dent Mater J 2012;31:523–7.
[8] Satterthwaite JD, Vogel K, Watts DC. Effect of resin-composite filler particle size and shape on shrinkage-strain. Dent Mater 2009;25:1612–5.
[9] Turssia CP, Ferracanea JL, Vogel K. Filler features and their effects on wear and degree of conversion of particulate dental resin composites. Biomaterials 2005;26:4932–7.
[10] Darvell BW. Metals I: structure. In: Materials science for dentistry. Cambridge and Florida: Woodhead Publishing Limited and CRC Press LLC; 2009, pp. 280–305.
[11] Callister WD, Rethwisch DG. The structure of crystalline solids. In: Materials science and engineering: an introduction. New York: John Wiley & Sons, Inc.; 2007, pp. 38–79.
[12] Woodcock LV. Entropy difference between the face-centred cubic and hexagonal close-packed crystal structures. Nature 1997;385:141–3.
[13] Sattler KD. Handbook of nanophysics: nanoparticles and quantum dots. Florida: CRC Press; 2016.
[14] Goertzen WK, Kessler MR. Dynamic mechanical analysis of fumed silica/cyanate ester nanocomposites. Compos A Appl Sci Manuf 2008;39:761–8.
[15] Badano JM, Betti C, Rintoul I, Berlanga JV, Cagnola E, Torres G, et al. New composite materials as support for selective hydrogenation; egg-shell catalysts. Appl Catal A Gen 2010;390:166–74.
[16] Ding T, Song K, Clays K, Tung CH. Fabrication of 3D photonic crystals of ellipsoids: convective self-assembly in magnetic field. Adv Mater 2009;21:1936–40.
[17] Brodu N, Dijksman JA, Behringer RP. Spanning the scales of granular materials through microscopic force imaging. Nat Commun 2015;6:6361.
[18] Owolabi TO, Akande KO, Olatunji SO. Estimation of surface energies of hexagonal close packed metals using computational intelligence technique. Appl Soft Comput 2015;31:360–8.
[19] Tilley RJD. Metals, ceramics, polymers and composites. In: Understanding solids: the science of materials. West Sussex: John Wiley & Sons, Inc.; 2004, pp. 139–188.
[20] Steward SA. An alternative description of hydrogen diffusion in the bcc metals. Solid State Commun 1975;17:75–8.
[21] Ellis AB, Geselbracht MJ, Johnson BJ, Lisensky GC, Robinson WR. Common crystalline structures. In: Teaching general chemistry: a materials science companion. USA: American Chemical Society; 1993, pp. 97–154.
[22] Petrucci RH, Harwood WS, Herring FG, Madura JD. Solids. In: General chemistry: principles & modern applications. USA: Prentice Hall; 2006, pp. 1068–1170.
[23] Delaney GW, Hilton JE, Cleary PW. Defining random loose packing for nonspherical grains. Phys Rev E 2011;83:051305.
[24] Henrich B, Wonisch A, Kraft T, Moseler M, Riedel H. Simulations of the influence of rearrangement during sintering. Acta Metall 2007;55:753–72.
[25] Onoda GY, Liniger EG. Random loose packings of uniform spheres and the dilatancy onset. Phys Rev Lett 1990;64:2727–30.
[26] Berryman JG. Random close packing of hard spheres and disks. Phys Rev A 1983;27:1053–61.
[27] Kamien RD, Liu AJ. Why is random close packing reproducible? Phys Rev Lett 2007;99:155501.
[28] Zamponi F. Mathematical physics: packings close and loose. Nature 2008;453:606–7.
[29] Gupta KM, Gupta N. Advanced electrical and electronics materials: processes and applications. In: Tiwari A, editor. Solid structures, characterization of materials, crystal imperfections, and mechanical properties of materials. Massachusetts and New Jersey: Scrivener Publishing LLC and John Wiley & Sons, Inc.; 2015, pp. 71–108.
[30] Wise H, Oudar J. Structural aspects. In: Material concepts in surface reactivity and catalysis. New York: Dover Publications, Inc.; 2012, pp. 1–24.
[31] Genovese DB. Shear rheology of hard-sphere, dispersed, and aggregated suspensions, and filler-matrix composites. Adv Colloid Interface Sci 2012;171–172:1–16.